THE EFFECT OF THE VERTICAL CANOPY STRUCTURE ON SNOW PROCESS: SIMULATIONS OF VERTICAL RESOLVED ENERGY FLUXES AND SNOW USING A HIGHER-ORDER CLOSURE MODEL

Laura McGowan[1], Kyaw Tha Paw U [1], Helen Dalhke[2], Shu-Hua Chen[1], and David Pyles[1]

ABSTRACT

Snow cover is a critical driver of the Earth's surface energy budget, climate change, and water resources. Variations in snow cover not only affect the energy budget of the land surface but also represent a major water supply source. In California, US estimates of snow depth, extent, and melt in the Sierra Nevada are critical to estimating the amount of water available both California agriculture, urban and environmental users. However, accurate estimates of snow cover and snowmelt processes in forested areas still remain a challenge. Canopy structure influences the vertical and spatiotemporal distribution of snow, and therefore ultimately determines the degree and extent by which snow alters both the surface energy balance and water availability in forested regions. In this study we use the Advanced Canopy Atmosphere Soil algorithm (ACASA), a multilayer soil vegetation atmosphere numerical model, to simulate the effect of different snow covered canopy structures on the energy budget, water budget, temperature and other scalar profiles within different forest types in the Sierra Nevada, California. ACASA incorporates a higher order turbulence closure scheme which allows the detailed simulation of turbulent fluxes of heat and water vapor as well as the CO_2 exchange of the within canopy layers. As such ACASA can capture the counter-gradient fluxes within canopies that may occur frequently, but are typically unaccounted for, in most snow hydrology models. Four different canopy types were modeled ranging from bottom heavy canopies with most of the biomass located near the ground to top heavy canopies with most of the biomass located near the top of the canopy. Preliminary results indicate that the canopy stand structure associated with the different canopy types fundamentally influence the vertical scalar profiles (including those of temperature, moisture, and wind speed) in the canopy and thus alter the interception and snow melt dynamics in the forested land surfaces. The differences in the vertical scalar profiles resulted in over one week difference in the complete melt of the seasonal below canopy snowpack between canopy types in high-snow scenarios. In addition, the turbulent transport dynamics, including counter-gradient fluxes are discussed in the context of the snow energy balance and potential misattribution of water sources within the vertical canopy that could occur when counter-gradient fluxes are not considered.
(KEYWORDS: snow, canopy interception, turbulence, counter-gradient fluxes)

INTRODUCTION

Canopy structure influences the vertical and spatiotemporal distribution of snow, and therefore ultimately determines the degree and extent by which snow alters both the surface energy balance and water availability in forested regions. Resolving the vertical canopy structure is critical to understanding canopy influence on snow dynamics; yet there are few studies explicitly resolving complex energy balance and water processes within multiple vertical canopy layers.

One common technique to study the impact of snow forest structure on the snow water and energy budgets has been to compare values at forested sites to open fields (Hardy et al., 1997; Mahat & Broxton, 2014; Harpold et al., 2014; Tarboton, 2014) or lakes (Harding & Pomeroy, 1996). Other studies investigate the influence of canopy structure on snow hydrology and energy by comparing unperturbed forests to forests perturbed by for example logging (Anderson & Gleason, 1960; Golding & Swanson, 1986; Berris & Harr, 1987; Schmidt & Troendle, 1989; Jost et al., 2009; Jost, et al., 2007; Koivusalo & Kokkonen, 2002; Murray & Buttle, 2003; Teti, 2003; Teti, 2008; Harpold et al., 2014; Mahat & Tarboton, 2014) mountain pine beetles (Boon, 2007; Teti, 2008; Pugh & Small 2011; Bewley et al., 2010; Pugh & Gordon, 2012; Pugh & Small 2013; Biederman et al., 2014; Winkler et al., 2014;

Paper presented Western Snow Conference 2016
[1]Laura McGowan: UC Davis, Atmospheric Science, Davis, CA, lemcgowan@ucdavis.edu
[1]Kyaw Tha Paw U: UC Davis, Atmospheric Science, Davis, CA, ktpawu@ucdavis.edu
[2]Helen Dalhke: UC Davis, Hydrology, Davis, CA, hdahlke@ucdavis.edu
[1]Shu-Hua Chen: UC Davis, Atmospheric Science, Davis, CA,shachen@ucdavis.edu
[1]David Pyles: UCD avis, Atmospheric Science, Davis, CA, rdpyles@gmail.com

Livneh et al., 2015; Welch et al., 2015) or wildfires (Harpold et al., 2014; Jin et al., 2012; Seibert et al., 2010; Teti 2003) . All of these studies that explore snow forest processes and structure influences typically only look at single layer parameters for the ground and/or above the canopy. The Advanced Canopy-Atmosphere-Soil algorithm (ACASA) model used in this study simulates latent heat, sensible heat, radiation fluxes, moisture fluxes, and temperatures for one hundred different positions within the canopy; ten within canopy layers each with their own ten leaf classes, of which there is one shaded class and 9 sunlit leaf angle classes (Pyles et al., 2000a). Furthermore, the ACASA model incorporates a higher order turbulence closure scheme that allows the detailed simulation of turbulent fluxes of heat and water vapor exchange of several layers within the canopy. Thus the model can capture the counter gradient fluxes within canopies that may occur frequently, but are typically unaccounted for in most snow hydrology models.

The combined literature on forest perturbation under snowy conditions have not been able to elucidate whether forest disturbances create a reduction in water availability because of more wind/sun exposure or an increased water availability due to the lack of snow interception (i.e., creating decreased canopy snow sublimation) and a step to resolving this question would be to use models that simulate processes related to complex forest structures (Broxton et al., 2014). Resolving the vertical structure of the canopy and energy budget terms could help explain the differences found in the literature. Furthermore the differences may have occurred because of differences in canopy structure at different sites that were not fully resolved.

Our research will mark the first snow hydrology study that we are aware of that uses an advanced multi-layer soil-vegetation-atmosphere numerical model, to simulate the effect of different snow-covered canopy structures on the energy and water budget within different forest types in the Sierra Nevada, California. Four different canopy types were modeled with ACASA, selected to have diverse vertical distribution of biomass: 1) fir (most biomass near the ground), 2) cedar (evenly distributed biomass along the vertical axis), 3) umbrella pine (top heavy biomass), and 4) grassland (no significant biomass above the ground). The results demonstrate that the canopy shape and structure associated with different canopy types fundamentally influence the vertical scalar profiles (including those of temperature, moisture, and wind speed) in the canopy which in turn alter the interception and snow melt dynamics of these forested land surfaces.

METHODS

The following section provides a description of ACASA. For more details on the ACASA model see Pyles et al. (2000) and for the basic structure behind ACASA (Meyers and Paw U, 1986; Meyers and Paw U, 1987).

Vertical Resolution

ACASA has an adjustable vertical resolution within the canopy and of the atmosphere above the canopy. For this study the simulations were run with the default setting of ten layers above and ten below the canopy (a total of 20 layers) as recommended to make certain that there are accurate calculations of vertical finite difference calculations with the top atmospheric layer extending to at least twice the canopy height (Pyles et al., 2000b). For each canopy layer there are ten leaf angle classes; nine of which are sunlit and one is shaded. Each leaf angle has its own leaf energy budget, temperature, physiology, and radiative transfer modeled numerically.

Temperature Calculations

ACASA has advanced and accurate temperature calculations for the leaf angles and stem surface in each layer, and the soil surface. The surface temperature is calculated with a 4^{th} order polynomial based on Paw U and Gao (1988) that is combined with the energy flux estimates (Pyles et al., 2000). It has been shown that this method greatly reduces errors compared to simpler calculations (reported errors of less than 0.1% for temperatures between 5 and 45 ^{0}C) (Paw U and Gao, 1988; Pyles et al., 2000).

Turbulence Closure

ACASA has a higher-order turbulence closure scheme to solve Reynolds averaged Navier-Stokes equations of motion and thermodynamic equations; the model explicitly accounts for both the production and dissipation of the third moments of turbulent perturbations, which are then used to calculate second moment terms such as the turbulent kinetic energy and the vertical turbulent transport of heat, mass and momentum (Pyles et al., 2000).

Energy Budget

ACASA calculates the within canopy radiative transfer for the visible, near infrared (NIR), and thermal bands (0.4 µm to 0.7 µm, 0.7 µm to 4.0 µm, 4.0 µm to 50.0 µm respectively). There are both direct and diffuse radiative calculations for the visible and near infrared bands. The radiative calculations for the shortwave bands are based on a modified equation from Meyers (1985). Thermal radiation in the model accounts for the changing leaf and soil surface temperatures (Pyles et al., 2000). The model also accounts for canopy heat-storage as the total of biomass, latent, and sensible heat storage (Pyles et al., 2000). Model iterations achieve a steady-state solution of the governing equations. Convergence occurs when the change in the energy flux at the top of the canopy is less than 0.5 Wm^{-2} over four iterations (Pyles et al., 2000).

Soil Moisture and Heat Transport

The model has a specified but adjustable number of soil layers with constant depths (4 to 20) and several root activity layers within the soil layers (Pyles et al., 2000). The number of soil layers was set to 4 in the model for this study based on previous, successfully simulations (Xu et al., 2014). Soil water content in the active root zone is controlled by via transpiration and evaporative losses. The surface evaporation, moisture and temperature of the soil are based on Ek and Mahart (1991) with additions to include the effect of soil humus content and fractional leaf litter cover and the attenuation of the soil thermal conductivity (Pyles et al., 2000).

Input Parameters

At each time step the ACASA simulations are forced with observed or simulated meteorological data at the top domain layer. The input meteorological variables are precipitation per time step (mm), specific humidity (g kg^{-1}) or relative humidity, mean wind speed (m s^{-1}), net radiation (Wm^{-2}) or downwelling shortwave radiation, downwelling long wave radiation (Wm^{-2}) (optional, if available), air temperature (Kelvin), atmospheric pressure (hPa), and CO_2 concentration (ppm). Thirty minute time steps were utilized in this study.

The soil model categorizes soil type based on 16 USDA NRCS classifications. The model can have 4-20 soil layers, a number of active root layers, a user-specified soil layer thickness. Other parameters needed for the model simulation that remain unchanged throughout the simulation are total leaf area index (LAI), canopy architecture, mean leaf canopy drag coefficient, and maximum ground PAR. Initialization is based on station data and where this is not possible the parameterizations were taken from default values in the literature.

ACASA: Canopy Structure

Within ACASA the user specifies the following canopy elements and physical properties: one-sided total leaf area index (m^2 m^{-2}), canopy architecture (Figure 1), leaf/canopy drag coefficient, canopy height (m), and maximum rubisco (umol m^{-2} s^{-1}), dry leaf PAR and NIR reflectivity, and canopy emissivity. There are seven predefined canopy architecture types.

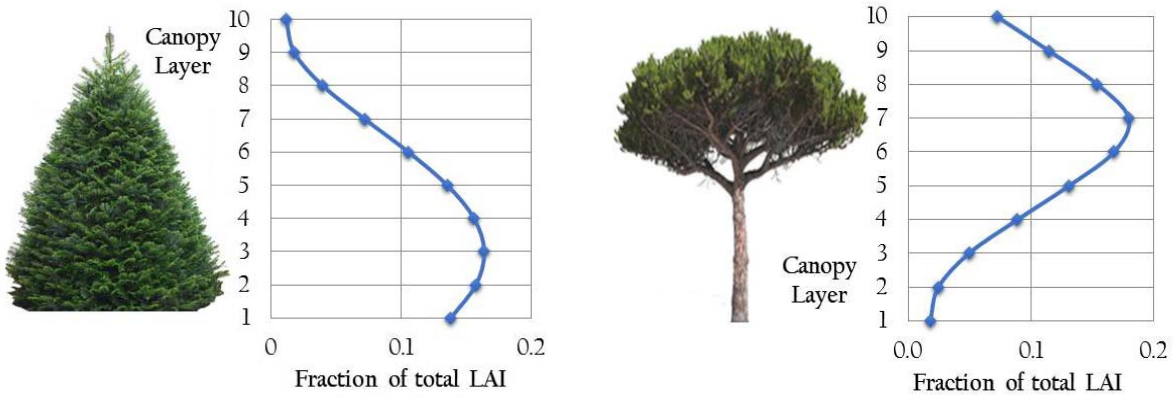

Figure 1. Examples of canopy architecture within ACASA. Plotted are canopy heights versus fraction of total LAI within the layer for a) conifer, b) umbrella pine.

ACASA: Snow Hydrology

Snow values are only output and determined from the energy budget and precipitation. Precipitation at the top of the canopy is either intercepted by the canopy or passes through the canopy to the ground. Snow intercepted by the canopy either evaporates or melts. Melt water from the canopy drips to the ground contributing to the throughfall classified as rain. The ground snowpack water equivalent is then calculated as the sum of snow throughfall minus ground snowpack evaporation and ground snowpack melt excluding ground snowpack meltwater refreeze (Figure 2).

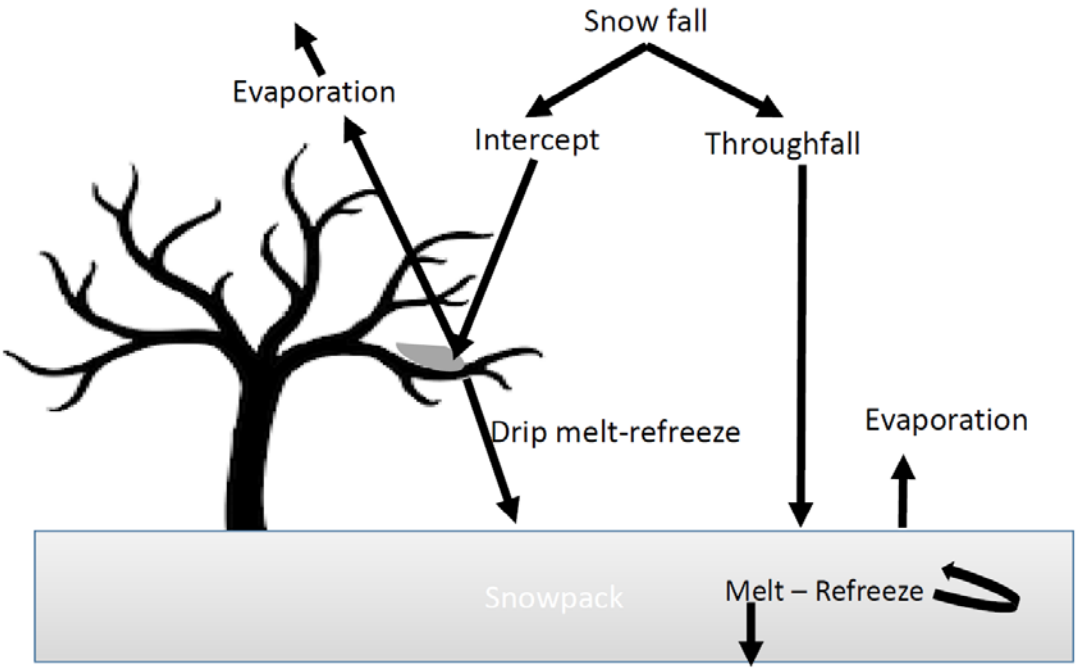

Figure 2. Simplified snow canopy and ground snowpack contribution overview. Canopy layers not shown.

Within Canopy Snow Mass Balance

Total canopy water content, W_C, at time step t is calculated with an energy mass balance approach. Where the total canopy water of the current time step is the sum of the snow water content in the previous time step plus any newly fallen snow intercepted by the canopy at the current time step, I_i, minus canopy evaporation/sublimation, Ec, and snow melt, M, excluding the fraction that refreezes, Rc (Koren et al., 1999). Mass release from canopy elements due to wind and increased temperatures is not yet considered. This is summed over summed over all canopy layers, i, and all leaf classes, j. Therefore for a given time step there are over 100 within canopy snow mass balance calculations.

$$\sum_{i,j}^{10} Wc_{i,j,t} = \sum_{i,j}^{10} Wc_{i,j,t-1} + \sum_{i,j}^{10} I_{i,j,t} - \sum_{i,j}^{10} Ec_{i,j,t} - \sum_{i,j}^{10} (M_{i,j,t} - Rc_{i,j,t}) \qquad (1)$$

Input precipitation at the top of the canopy is classified as snow when the air temperature is less than 0C and for all other air temperatures it is classified as rain. Model snow and rain interception occur at different rates and are calculated separately. The snow interception by the canopy is simply taken to be a fraction of the falling precipitation following Andreadis et al. (2009). The fraction of precipitation or dew that is intercepted remains on the leaves until it is evaporated or melts.

Evaporation from the surface and the canopy is calculated from the surface water flux which uses the Paw U and Gao's (1988) quartic technique, in equations 2 and 3 below. w'q' is the vertical kinematic eddy moisture

flux, ρ_w is the density of water, r_a is the aerodynamic resistance (s m^{-1}) for leaves, and r_s is the stomatal resistance (s m^{-1}) for leaves. When the canopy water content of a layer is non-zero, separate calculations for flux partitioning under free-evaporation conditions are performed. The resulting flux divergence estimates are then weighted by the fraction of the intercepted water to the maximum capacity within each layer (Pyles et al., 2000b).

$$w'q' = \frac{e_s - e_a}{r_a + r_s} \qquad (2)$$

$$E_c = \frac{w'q'}{\rho_w} \qquad (3)$$

Ground Snowpack Mass Balance

Ground snowpack total water equivalent, W_g, in meters, at time step t is calculated using the following mass balance approach;

$$W_{g_t}\rho_w = W_{g_{t-1}}\rho_w + H - E_g - (M_g - X_g) \qquad (4)$$

The variables are defined in the following manner, H is throughfall (m), E_g is evaporation/ablation from the ground snowpack (m), M_g is the sum of the melt from the top and bottom of the ground snowpack (m), and X_g refreeze of melt water within the ground snowpack (m). Throughfall, H, (m) is defined as snowfall at the top of the canopy minus the total snowfall that has been intercepted by the canopy.

Snowpack Density

Snow density calculations were based on equation 7 and 8 from Koren et al. (1999). The density equation from Koren et al. (1999) accounts for compaction of the snowpack over time. Snow density increases depending on snow water amount above level z and snow temperatures at that level in this method.

Meteorological Input Data and Quality Control

The required meteorological data were provided by Fluxnet Blodgett Sound Station (http://fluxnet.ornl.gov/site/826) located at 38.895° N, -120.632°W. The site elevation is 1330 meters but the data were extrapolated to a height of 2000 meters to be more representative of the nearby elevation of SNOTEL stations within the Sierras. Simulations were run for the winter of 2000 to 2001, a slightly below average snow season in the Sierras. Only time periods without large missing data gaps were used as input for the model. Basic data quality control was performed on the data including setting negative precipitation values as missing data and filling data with gaps of less than one hour by linear interpolation from the previous and next available time steps. Means and standard deviations were also investigated to eliminate spurious data where precipitation values greater than 5 standard deviations were flagged. Temperatures maximum, minimums, or averages greater than absolute value of 30°C were marked for further inspection. In addition, if the temperature maximum, minimums, or averages were identical for more than three days in a row the data were marked (Serreze et al., 1999).

RESULTS AND DISCUSSION

A primary impact of the vertical canopy structure is to determine the vertical displacement of snow. ACASA is able to capture vertical variations in snow cover within the canopy (Figure 3). For most temporal periods, there is a high correlation between the distribution of the snow within the canopy and the vertical distribution of biomass. The canopy of the fir retains most of the snow towards the base of the canopy and the umbrella pine stores most of the snow near the top of the canopy.

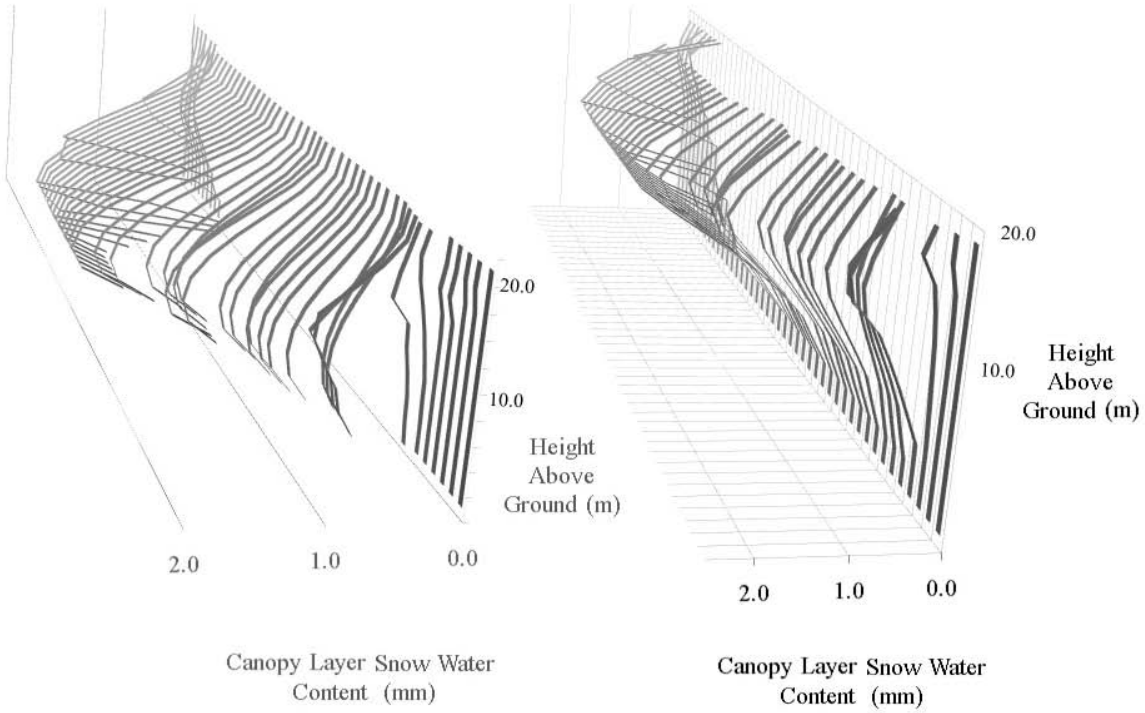

Figure 3. Vertical profiles of SWE distribution within a) fir, right, and b) umbrella pine canopy, left, for a 24 hour period. The x-axis indicates the height above ground in meters, and the y-axis shows the 30-minute time steps progressing forward in time from left to right, and the z-axis is the snow water equivalent held in a given canopy layer reported in millimeters.

The different distribution of snow in the vertical resulted in differences in the timing of the snowmelt release. The top-heavy canopies melted the entire beneath-canopy snowpack before bottom-heavy canopies. The loss of the snowpack first occurs in the umbrella pine, then the cedar, and finally in the pine. The length of the melt period was compared to the grassland control which had the longest melt period. The melt period of the umbrella pine was 18 days shorter than the grassland and 6 days shorter than the melt period of the fir. The shorter melt period of the umbrella pine is due to smaller beneath canopy snow accumulation and faster melt rate. During the melt period the snowpack beneath the umbrella pine was approximately 20 cm less than the snowpack beneath the Fir. The difference in snow accumulation occurred because of larger total evaporation and sublimation beneath the umbrella pine canopy (and fraction as percent of interception). The difference in the onset of melt implies quantitative models need to start considering the vertical distribution of snow more readily by either modeling energy and water fluxes within multiple canopy layers or by parameterization to accurately predict snowmelt water release.

Counter-gradient fluxes occurred frequently within the simulation. The graph shows an example of one counter-gradient flux that occurred within the fir canopy (Figure 4). The dual gradient within the canopy, with the top of the canopy having condensation occurring and the bottom canopy evaporating could potential imply that the upper canopy is graining water mass from the lower canopy. If this event was misrepresented by a single gradient model typical of most hydrology models it could potentially underestimate snow loss from the bottom of the canopy and the ground snowpack as it would only see a single negative latent heat flux.

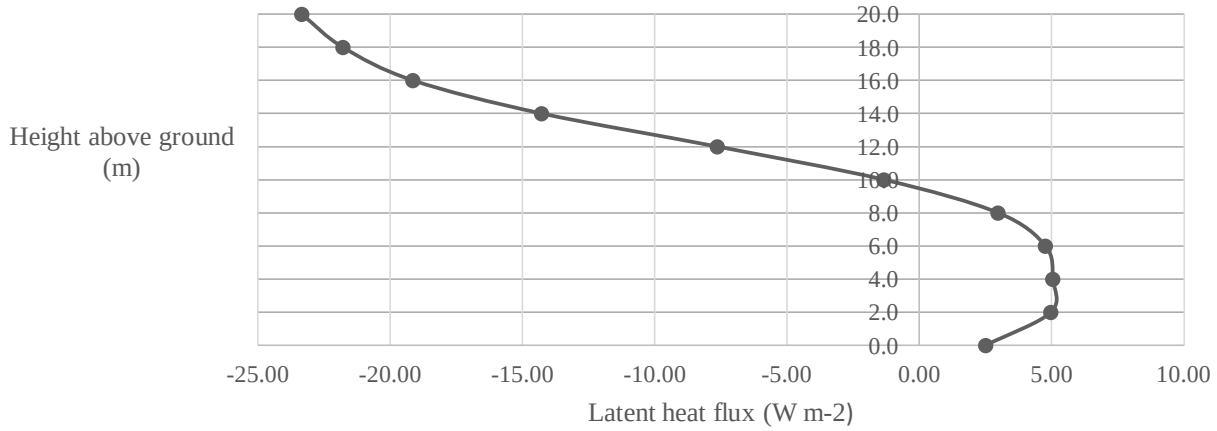

Figure 4. The y axis is the height above the ground in meters and the x axis the latent heat flux in W m^{-2}. Negative values of latent heat represent condensation, a gain in water mass, and positive values represent evaporation or sublimation, a loss of water.

CONCLUSION

The effect of vertical canopy structure on snow processes was examined utilizing the high-order closure model ACASA. Four different canopy types were modeled ranging from bottom heavy canopies with most of the biomass located near the ground to top-heavy canopies with most of the biomass located near the top of the canopy. The model captures the different vertical distribution of snow which generally correlates with biomass distribution. Different canopy structures resulted in different duration of snowmelt; with top-heavy canopies having the shortest snow melt period and the largest canopy evaporation and sublimation. Lastly, counter-gradient fluxes frequently occurred and their significance should be considered to potentially avoid misattribution and estimation errors.

REFERENCES

Anderson, H. W., and C. H. Gleason. 1960. Effects of logging and brush removal on snow water runoff. *International Association of Hydrologic Science Publication*, **51,** 478-489.

Andreadis, K. M., P. Storck, and D. P. Lettenmaier. 2009. Modeling snow accumulation and ablation processes in forested environments. *Water Resources Research*, **45**, W05429.

Berris, S. N., and R. D. Harr. 1987. Comparative snow accumulation and melt during rainfall in forested and clear-cut plots in the western Cascades of Oregon. *Water Resources Research*, **23,** 135-142.

Bewley, D., Y. Alila, and A. Varhola. 2010. Variability of snow water equivalent and snow energetics across a large catchment subject to Mountain Pine Beetle infestation and rapid salvage logging. *Journal of Hydrology*, **388,** 464-479.

Biederman, J. A., and Coauthors. 2014. Multiscale observations of snow accumulation and peak snowpack following widespread, insect-induced lodgepole pine mortality. *Ecohydrology*, **7,** 150-162.

Boon, S. 2007. Snow accumulation and ablation in a beetle-killed pine stand in Northern Interior British Columbia. *Journal of Ecosystems and Management*, **8**, 1-13.

Broxton, P. D., A. A. Harpold, J. A. Biederman, P. A. Troch, N. P. Molotch, and P. D. Brooks. 2014. Quantifying the effects of vegetation structure on snow accumulation and ablation in mixed-conifer forests. *Ecohydrology*, **8**,1073-1094.

Ek, M., and L. Mahart. 1991. OSU 1-D PBL Model User's Guide: a one-dimensional plantetary boundary layer model.

Golding, D. L., and R. H. Swanson. 1986. Snow distribution patterns in clearings and adjacent forest. *Water Resources Research*, **22,** 1931-1940.

Harding, R. J., and J. W. Pomeroy. 1996. The Energy Balance of the Winter Boreal Landscape. *Journal of Climate*, **9,** 2778-2787.

Hardy, J., R. Davis, R. Jordan, X. Li, C. Woodcock, W. Ni, and J. McKenzie. 1997. Snow ablation modeling at the stand scale in a boreal jack pine forest. *Journal of Geophysical Research: Atmospheres (1984–2012)*, **102,** 29397-29405.

Harpold, A. A., and Coauthors. 2014. Changes in snow accumulation and ablation following the Las Conchas Forest Fire, New Mexico, USA. *Ecohydrology*, 7, 440-452.

Jin, Y., J. T. Randerson, S. J. Goetz, P. S. A. Beck, M. M. Loranty, and M. L. Goulden. 2012. The influence of burn severity on postfire vegetation recovery and albedo change during early succession in North American boreal forests. *Journal of Geophysical Research: Biogeosciences*, **117,** G01036.

Jost, G., M. Weiler, D. R. Gluns, and Y. Alila. 2007. The influence of forest and topography on snow accumulation and melt at the watershed-scale. *Journal of Hydrology*, **347,** 101-115.

Jost, G., R. D. Moore, M. Weiler, D. R. Gluns, and Y. Alila. 2009. Use of distributed snow measurements to test and improve a snowmelt model for predicting the effect of forest clear-cutting. *Journal of Hydrology*, **376,** 94-106.

Koivusalo, H., and T. Kokkonen. 2002. Snow processes in a forest clearing and in a coniferous forest. *Journal of Hydrology*, **262,** 145-164.

Koren, V., J. Schaake, K. Mitchell, Q. Y. Duan, F. Chen, and J. Baker. 1999. A parameterization of snowpack and frozen ground intended for NCEP weather and climate models. *Journal of Geophysical Research*: *Atmospheres* (1984–2012), 104, 19569-19585.

Livneh, B., and Coauthors. 2015. Catchment response to bark beetle outbreak and dust-on-snow in the Colorado Rocky Mountains. *Journal of Hydrology*, **523,** 196-210.

Mahat, V., and D. G. Tarboton. 2014. Representation of canopy snow interception, unloading and melt in a parsimonious snowmelt model. *Hydrological Processes*, **28,** 6320-6336.

Meyers, T., and K.T. Paw U. 1986. Testing of a higher-order closure model for modeling airflow within and above plant canopies. *Boundary-Layer Meteorology*, **37**, 297-311.

Meyers, T. P. 1985. A simulation of the canopy microenvironment using higher order closure principles. PhD dissertation, Purdue University, West Lafayette, IN.

Meyers, T. P., and K. T. Paw U. 1987. Modelling the plant canopy micrometeorology with higher-order closure principles. *Agricultural and Forest Meteorology*, **41**, 143-163.

Murray, C. D., and J. M. Buttle. 2003. Impacts of clearcut harvesting on snow accumulation and melt in a northern hardwood forest. *Journal of Hydrology*, **271,** 197-212.

Musselman, K. N., N. P. Molotch, S. A. Margulis, P. B. Kirchner, and R. C. Bales. 2012. Influence of canopy structure and direct beam solar irradiance on snowmelt rates in a mixed conifer forest. *Agricultural and Forest Meteorology*, **161,** 46-56.

Paw U, K. T., and W. Gao. 1988. Applications of solutions to non-linear energy budget equations. *Agricultural and Forest Meteorology*, **43**, 121-145.

Pugh, E., and E. Small. 2012. The impact of pine beetle infestation on snow accumulation and melt in the headwaters of the Colorado River. *Ecohydrology*, **5,** 467-477.

Pugh, E., and E. Gordon. 2013. A conceptual model of water yield effects from beetle-induced tree death in snow-dominated lodgepole pine forests. *Hydrological Processes*, **27,** 2048-2060.

Pugh, E. T., and E. E. Small. 2013. The impact of beetle-induced conifer death on stand-scale canopy snow interception. *Hydrol. Res*, **44**, 644-657.

Pyles, D., B. Weare, and K. T. Paw U. 2000. The UCD Advanced Canopy-Atmosphere-Soil Algorithm: Comparisons with observations from different climate and vegetation regimes. *Quarterly Journal of the Royal Meteorological Society*, **126**, 2951-2980.

Schmidt, R. A., and C. A. Troendle. 1989. Snowfall into a forest and clearing. *Journal of Hydrology*, **110,** 335-348.

Seibert, J., J. J. McDonnell, and R. D. Woodsmith. 2010. Effects of wildfire on catchment runoff response: a modelling approach to detect changes in snow-dominated forested catchments. *Hydrology res*, **41**, 378-390.

Tarboton, D. G., and C. H. Luce. 1996. *Utah energy balance snow accumulation and melt model (UEB).* Citeseer.

Teti, P., 2003. Relations between peak snow accumulation and canopy density. *The Forestry Chronicle*, **79,** 307-312.

Teti, P. A. 2008. Effects of overstory mortality on snow accumulation and ablation. Natural Resources Canada, Canadian Forest Service, Pacific Forestry Centre, Victoria, BC. Mountain Pine Beetle Working Paper 2008-13. 34 p.

Varhola, A., N. C. Coops, Y. Alila, and M. Weiler. 2014. Exploration of remotely sensed forest structure and ultrasonic range sensor metrics to improve empirical snow models. *Hydrological Processes*, **28,** 4433-4448.

Welch, C. M., P. C. Stoy, F. A. Rains, A. V. Johnson, and B. L. McGlynn. 2016. The impacts of mountain pine beetle disturbance on the energy balance of snow during the melt period. *Hydrological Processes*, **30**, 588-602.

Winkler, R., S. Boon, B. Zimonick, and D. Spittlehouse. 2014. Snow accumulation and ablation response to changes in forest structure and snow surface albedo after attack by mountain pine beetle. *Hydrological Processes*, **28,** 197-209.

Xu, L., R. D. Pyles, K. T. Paw U, S. H. Chen, and E. Monier. 2014. Coupling the high-complexity land surface model ACASA to the mesoscale model WRF. *Geosci. Model Dev.*, **7**, 2917-2932.